Journal of Macromolecular Science, Part A
Publication details, including instructions for authors and subscription information:
http://www.informaworld.com/smpp/title~content=t713597274

Synthesis and Catalytic Activity of Polymer Supported Schiff Base Complexes of Copper(II) and Iron(III) Ions in Comparison to Unsupported Complexes

K. C. Gupta[a]; H. K. Abdulkadir[a]
[a] Polymer Research Laboratory, Department of Chemistry, Indian Institute of Technology, Roorkee, India

To cite this Article Gupta, K. C. and Abdulkadir, H. K.(2008) 'Synthesis and Catalytic Activity of Polymer Supported Schiff Base Complexes of Copper(II) and Iron(III) Ions in Comparison to Unsupported Complexes', Journal of Macromolecular Science, Part A, 45: 1, 53 — 64

To link to this Article: DOI: 10.1080/10601320701683256

URL: http://dx.doi.org/10.1080/10601320701683256

Journal of Macromolecular Science®, Part A: Pure and Applied Chemistry (2008) **45**, 53–64

ISSN: 1060-1325 print/1520-5738 online
DOI: 10.1080/10601320701683256

Synthesis and Catalytic Activity of Polymer Supported Schiff Base Complexes of Copper(II) and Iron(III) Ions in Comparison to Unsupported Complexes

K. C. GUPTA and H. K. ABDULKADIR

Polymer Research Laboratory, Department of Chemistry, Indian Institute of Technology, Roorkee, India

Received June, 2007, Accepted July, 2007

The polymer supported metal complexes of N,N′-bis(acetyl acetone)o-phenylene-diamine (ACPDA) Schiff base were synthesized by suspension copolymerization of styrene and allyl chloride in the presence of divinyl benzene (DVB) as cross-linker and azobisisobutyronitrile (AIBN) as initiator at 70 ± 0.1°C and then ACPDA Schiff base and metal ions were loaded on the resulting polymer beads. The cross-linked density in polymer beads was varied by taking different concentrations of divinyl benzene in the reaction mixture. The polymer beads were characterized for their cross-linked density, size (ϕ), density (ρ), degree of swelling ($\%S_w$) and loading of ACPDA Schiff base and metal ions. The polymer beads prepared with 1.5 mmol of DVB (Type III) had a sufficient amount of allyl chloride (4.90 mmol, 0.367 g) and showed optimum loading for ACPDA Schiff base (1.96 mmol g^{-1}) and metal ions. The structures of copper(II) and iron(III) ions complexes (ACPDA-M) and their loading on polymer beads (P-ACPDA-M) was characterized with spectral analysis. The catalytic activity of unsupported and polymer supported ACPDA Schiff base complexes of copper(II) and iron(III) ions was evaluated by studying the rate of decomposition of hydrogen peroxide.

The rate of decomposition (Rp) of hydrogen peroxide varied linearly with a concentration of hydrogen peroxide and catalyst, but varied inversely with hydrogen ions concentration. Finally reaction steps for decomposition of H_2O_2 were proposed and a rate expression was derived considering the experimental data.

Keywords: allyl chloride; styrene; catalysis; cross-linking; polymer support

1 Introduction

The synthesis of various β-diketones and their coordination ability with metal ions is reported (1). The reported metal complexes of β-diketones are either high spin octahedral or low spin square planar in their structures (1, 2). Although these investigations were primarily aimed to establish the geometry of metal complexes of β-diketones, but subsequent studies were made to evaluate their catalytic activities in homogeneous and heterogeneous conditions (3). The titanium complexes of β-diketones were syndiotactic and showed catalytic activity in polymerization of styrene (4). The polymer supported metal complexes of β-diketones were more active in epoxidation of alkenes than their unsupported analogues. These investigations have clearly indicated that polymer supported catalysts were more efficient in substrate conversion and selectivity of the products (5, 6) than homogeneous catalysts. The polymer bound catalysts are more suitable for industrial processes than unsupported catalysts due to their ease of separation from reaction mixture and a high turnover number (7–12). The microenvironment (13) and degree of cross-linking (14) in polymer supports was responsible to control the activity of metal complexes. The cross-linked polymers were more efficient in controlling the activity of metal complexes than linear polymers (15, 16) as linear polymers were not able to influence the concentration of reactants on active sites as influenced by cross-linked polymers. The polymer backbone flexibility is one of the factors for better catalytic activity of metal complexes on polymer supports in comparison to inorganic supports (17–20). Cross-linked polymer supports have shown a remarkable effect on activity (21–23), and selectivity (24–26) of metal complexes, which is barely observed with soluble (27) and inorganic supports (17, 20) such as zeolites (28). The efficiency of polymer supports was modified further using a spacer between metal complex and polymer backbone (29–31) for stereospecific interactions between metal complexes and reactants. The activity of 1, 3-diketonato

---

Address correspondence to: K. C. Gupta, Polymer Research Laboratory, Department of Chemistry, Indian Institute of Technology, Roorkee 247 667, India. Tel.: +91 1332 285325; Fax: +91 1332 286202; E-mail: kcgptfcy@iitr.ernet.in

metal complexes was enhanced by enolization (32, 33) for syndiotactic polymerization of styrene (34, 35). The catalytic activity of these 1,3-diketonato complexes on polymer supports was higher (36) than in solution. The synthesis of metal complexes of N,N′-bis (acetyl acetone) o-phenylene diamine Schiff base and their catalytic activity is not reported in the literature; hence, in these investigations, efforts were made to prepare polymer supported N,N′-bis (acetyl acetone) o-phenylene diamine Schiff base complexes of copper(II) and iron(III) ions and characterized for their structures and catalytic activity in decomposition of hydrogen peroxide.

2 Experimental

2.1 Materials

Acetylacetone with a boiling range of 132°C–135°C was obtained from Loba Chemie, Mumbai, India. The styrene (St) and divinyl benzene (DVB) were received from Aldrich Chemical Company, USA, and used without further purification.

2.2 Spectral and Magnetic Measurements

ACPDA Schiff base and its metal complexes (M-ACPDA) were characterized by recording their I.R. spectra on KBr pellets using a Perkin-Elmer 1600 FT-IR Spectrophotometer. The electronic spectra of ACPDA Schiff base and its metal complexes were recorded using a UV-vis 1601 PC Shimadzu Spectrophotometer. The magnetic moment (μ) of metal complexes was recorded using a Gouy Balance at 294 K and used to determine the electronic state of metal complexes.

2.3 Thermal Analysis

Thermal stability of polymer supported Schiff base (P-ACPDA) and its metal complexes (P-ACPDA-M) was determined using a Stanton Red Croft STA-780 Thermal Analyzer (UK) at a heating rate of 10°C/min under nitrogen atmosphere.

2.4 Elemental Analysis

The composition of APDA Schiff base and its metal complexes (M-ACPDA) was determined by elemental analysis using a Perkin-Elmer 240 Elemental Analyzer.

2.5 Molecular Weight Measurements

Molecular weight of ACPDA Schiff base and its metal complexes (M-ACPDA) was determined using a Vapor Pressure Osmometer (Knauer K-700, Germany) and benzil as the standard.

2.6 SEM Analysis

The size of cross-linked polymer beads was determined using a Scanning Electron Microscope (Leo-435, VP, England) by mounting polymer beads on metal studs with double adhesive tapes and vacuum coating with gold.

2.7 Degree of Swelling and Pore Volume in Polymer Beads

The degree of swelling (S_w) in cross-linked polymer beads was determined by soaking beads for 24 h in dimethyl formamide (DMF) and determining their weight (W_t) in comparison to their initial weight (W_0) for fitting in Equation (1.) The pore volume (V_p) in polymer beads was determined using initial (W_0) and final weights (W_t) after immerging polymer beads for 24 h in DMF and using Equation (2).

$$S_w = \frac{W_t - W_0}{W_0} \times 100 \tag{1}$$

$$V_p = \frac{W_t - W_0}{W_0 \cdot d_B} \times 100 \tag{2}$$

Where, d_B is the density of DMF.

2.8 Density of Polymer Beads

The density of polymer beads (ρ) was determined by a liquid displacement technique (ASTM-792) using Equation (3).

$$\rho = \left(\frac{W_0}{W_a + W_h - W_b}\right) 0.9975\,\mathrm{g\ cm^{-3}} \tag{3}$$

Where, W_a is the weight of polymer beads in air, whereas W_h is the weight of beads immerged completely and partially immerged holder in the liquid. W_b is the weight of totally immersed holder in the liquid.

2.9 Loading of Metal Ions

The loading of metal ions on polymer supported N,N′-bis (acetyl acetone) o-phenylene diamine Schiff base (P-ACPDA) was determined by estimating the amount of metal ions loaded on polymer beads using a Perkin-Elmer 2100 Atomic Absorption Spectrometer at a characteristic wave length (λ_{max}) of metal ions.

2.10 Polymerization of Styrene and Allyl Chloride

The cross-linked polymer beads were synthesized by suspension polymerization of styrene (48.97 mmol, 5.1 g), allyl chloride (48.97 mmol, 3.746 g) and divinyl benzene (1.5 mmol, 0.195 g) in the presence of gelatin (0.75 g), bentonite (2.0 g), boric acid (2.5 g) and polyvinyl alcohol (1.5 g) in a three-necked round bottom flask containing 500 mL water. The solution was deaerated with nitrogen gas and polymerization was initiated by adding 10 mL deaerated solution of azobisisobutyronitrile (9.4×10^{-4} mmol, 0.15 g) in the flask. After 6 h, the heating of reaction mixture was stopped and the solution was allowed to cool under continuously stirring. Finally, the polymer beads were separated and washed with methanol to remove unreacted monomer and other impurities. The beads of different cross-linked densities were synthesized by varying the amount of DVB from 0.8–2.0 mmol in the reaction mixture. The variation in DVB in the reaction mixture also controlled the amount of allyl chloride in polymer beads. The polymer beads were characterized for density (ρ), degree of swelling (S_w) and pore volume (V_p).

2.11 Crosslinked Molecular Weights (M_C)

Cross-linked molecular weight (M_c) was determined in polymer beads prepared at different concentrations of divinyl benzene (DVB) by using Equation (4).

$$M_c = 3\,\frac{\rho \mathrm{RT}}{\mathrm{E}}(\phi_2)^{1/3} \tag{4}$$

Where, E is the Young's modulus of polymer and ϕ_2 is the volume fraction of polymer.

2.12 Synthesis of N,N′-bis (acetyl acetone) o-Phenylene Diamine Schiff Base and its Metal Complexes

The N,N′-bis(acetyl acetone) o-phenylene diamine Schiff base (ACPDA) was prepared by refluxing o-phenylene diamine (5 mmol, 0.54 g) and acetyl acetone (10 mmol, 1.0 g) in 20 mL benzene at 60°C for 6 h. The resultant Schiff base was separated from the reaction mixture and recrystallized from ethanol. The Schiff base was characterized for its structures and molecular weight by elemental and spectral analysis. The metal complexes of Schiff base (M-ACPDA) were prepared by refluxing Schiff base (5 mmol, 1.36 g) at 60°C–70°C in a 20 mL solution of metal ions (5 mmol). After 8 h, the reaction mixture was cooled and precipitated metal complexes were recrystallized from ethanol.

2.13 Synthesis of Polymer Supported Schiff Base and its Metal Complexes

N,N′-bis (acetyl acetone) o-phenylene diamine (ACPDA) Schiff base was supported on DMF swollen polymer beads of different cross-linked density by refluxing ACPDA Schiff base at 60°C–70°C in DMF solution. After refluxing for 8 h, the Schiff base supported polymer beads (P-ACPDA) were separated and dried in vacuum oven at 60°C after washing with DMF and methanol. The amount of ACPDA Schiff base supported on polymer beads was estimated with elemental analysis and I.R. spectra were used as evidence for anchoring the Schiff base. The loading of metal ions was carried out by refluxing Schiff base supported polymer beads (1.0 g) at 70°C in 40 mL DMF containing a known amount of metal ions (8 mmol). After 8 h, the polymer beads were separated and dried in a vacuum oven after washing with hot and cold water. The solution was analyzed by atomic absorption spectrometer to determine the amount of metal ions loaded on polymer beads. The complexation of metal ions with polymer supported Schiff base was confirmed by comparing the I.R. spectra of metal ions loaded polymer beads (P-ACPDA-M) with I.R. spectra of Schiff base supported polymer beads (P-ACPDA). The comparison of UV spectra of polymer supported metal complexes with unsupported metal complexes was used to analyze the influence of polymer matrix on structures of metal complexes.

The efficiency of complexation (%EC) and efficiency of loading (%EL) of metal ions on ACPDA Schiff base supported polymer beads was determined using Equations (5) and (6).

$$\%\mathrm{EC} = \frac{\text{Amount of metal ions loaded g}^{-1}\text{of beads}}{\text{Amount of Schiff base loaded g}^{-1}\text{of beads}} \times 100 \tag{5}$$

$$\%\mathrm{EL} = \frac{\text{Amount of metal ions loaded g}^{-1}\text{of beads}}{\text{Amount of metal ions used for loading}} \times 100 \tag{6}$$

The loading of Schiff base and metal ions on polymer beads was determined as a function of degree of cross-linking and type of metal ions.

2.14 Evaluation of Catalytic Activity of Unsupported and Polymer Supported Schiff Base Complexes of Copper(II) and Iron(III) Ions

The effect of polymer support on catalytic activity of metal complexes was determined by studying the decomposition of hydrogen peroxide in the presence of unsupported and polymer supported metal complexes of ACPDA Schiff base. The decomposition of hydrogen peroxide was followed by estimating the remaining amount of hydrogen peroxide with potassium permanganate (0.01 M) in the presence of sulfuric acid (0.01 M). The activity of complexes of copper(II) and iron(III) ions was determined at different concentrations of hydrogen peroxide and using different concentrations of unsupported and polymer supported metal complexes of ACPDA Schiff base. The energy of activation (Ea) for decomposition of hydrogen peroxide was determined using rate constant (k) determined for decomposition of hydrogen peroxide at different temperatures. The effect of polymer support on activity of catalysts was determined by comparing the energy of activation for decomposition of hydrogen peroxide determined with unsupported and polymer supported Schiff base complexes of metal ions. The effect of solution pH on activity of the catalyst in decomposition of hydrogen peroxide was also analyzed by studying the rate of decomposition of hydrogen peroxide in a solution of different pH (37).

Table 1. Physical characteristics of divinyl benzene (DVB) cross-linked polymer beads

Types of beads	$[DVB]_I$/ mmol	Beads size ϕ/μm	ρ/g cm^{-3}	Sw (%)	Pore volume/cm^3 g^{-1}	Cross-link M_C/kg mol^{-1}
I	0.80	214.0	0.39	8.65	0.62	1.53
II	1.15	208.0	0.42	6.23	0.52	1.40
III	1.50	205.0	0.46	4.83	0.48	1.35
IV	1.75	201.0	0.48	4.02	0.42	1.10
V	2.00	196.0	0.52	3.90	0.21	0.90

$[Styrene]_I = 48.97$ mmol, $[Allyl\ chloride]_I = 48.97$ mmol.

3 Results and Discussion

The physical characteristics of synthesized polymer beads varied with the amount of divinyl benzene (DVB) used as cross-linker (Table 1). The divinyl benzene controlled the degree of cross-linking and the amount of allyl chloride. The amount of Schiff base supported on polymer beads varied with available active sites (7) and physicochemical properties of polymer beads (14–16). Allyl chloride in polymer beads controlled the amount of supported Schiff base. The presence of allyl chloride in synthesized polymer beads was confirmed due to the presence of additional absorption band at 1262 cm^{-1} in I.R spectra of polymer beads (38) in comparison to I.R. spectra of polystyrene.

The polymer beads obtained at 1.5 mmol of divinyl benzene (Type III) contained 4.90 mmol of allyl chloride as confirmed from the content of chlorine (Cl, 17.40 wt.%) as determined by elemental analysis. The amount of allyl chloride varied from 5.80 mmol g^{-1} to 4.46 mmol g^{-1} in polymer beads, which were obtained on varying the concentration of divinyl benzene from 0.8 mmol to 2.0 mmol (Table 2). The amount of allyl chloride in the polymer beads has ultimately controlled the loading of metal ions by controlling the amount of polymer supported Schiff base.

The loading of Schiff base and metal ions varied with cross-link molecular weights (M_c) and by the amount of allyl chloride present in the beads (Tables 1 and 2). The cross-linked molecular weights (M_c) is a significant factor in controlling the accessibility of Schiff base to react with pendant chlorine in polymer beads. The substantial decrease in cross-linked molecular weights (M_C) at high concentration of divinyl benzene (>1.5 mmol) has decreased the diffusion and complexation of metal ions (Table 3). The synthesized polymer beads were more flexible in comparison to conventionally used cross-linked chloromethylated polystyrene beads, which might be due to the presence of allyl chloride blocks in between rigid blocks of polystyrene; hence, these polymer beads were more flexible and showed an optimum degree of swelling (Figure 1) and loading of Schiff base in dimethyl formamide. The synthesized polymer beads were suitable for loading of Schiff base and metal ions due to facile orientations of N_2O_2 donor sites of supported acetyl acetone (39).

Since the loading of Schiff base and metal ions showed variation with properties of polymer beads; hence, polymer beads obtained at different concentrations of divinyl benzene were characterized for various parameters, which played a significant role in loading of metal ions and activity of metal complexes (Table 1). The size of polymer beads varied from 214 μm to 196 μm, varying the concentration of divinyl benzene from 0.8–2.0 mmol (Table 1). A deceasing trend in the size of polymer beads on increasing the concentration of divinyl benzene was due to the increase in degree of cross-linking between polymer chains, which is evident from the variation in cross-link molecular weights (M_c) from 1.53 kg mol^{-1} to 0.90 kg mol^{-1} (Table 1). The polymer beads showed variations in density (ρ) and pore volume (V_p) on varying the amount of divinyl benzene. The density (ρ) of polymer beads varied from 0.39–0.52 g cm^{-3} and pore volume (V_p) from 0.62–0.21 cm^3 g^{-1} on varying the concentration of DVB from 0.8 mmol to 2.0 mmol in the reaction mixture (Table 1).

Table 2. Composition of Schiff base (ACPDA) supported cross-linked polymer beads

Types of beads	% Cl in beads	ACL in beads/ mmol g^{-1}	% N in beads	Schiff base in beads/ mmol g^{-1}	% Cl* in beads	Free ACL in beads/ mmol g^{-1}
I	20.59	5.80	4.36	1.52	9.80	2.76
II	18.18	5.10	5.23	1.84	5.20	1.46
III	17.40	4.90	5.32	1.96	3.48	0.98
IV	17.04	4.80	4.88	1.70	4.97	1.40
V	15.83	4.46	4.20	1.46	5.54	1.54

$[Styrene]_I = 48.97$ mmol, $[ACL]_I = 48.97$ mmol, $[ACPDA]_I = 5.0$ mmol, (*in ACPDA loaded beads).

Table 3. Efficiency of loading (%EL) and complexation (%EC) of metal ions (M) on Schiff base (ACPDA) supported cross-linked polymer beads

Types of beads	Schiff base in beads/ mmol g^{-1}	Loading of copper(II) ions			Loading of iron(III) ions		
		mmol g^{-1}	%EL	%EC	mmol g^{-1}	%EL	%EC
I	1.52	0.85	17.02	56.0	0.94	18.70	61.5
II	1.84	1.23	24.64	67.0	1.44	28.84	78.4
III	1.96	1.38	27.57	70.4	1.71	34.20	87.2
IV	1.70	1.02	20.40	60.0	1.21	24.14	71.0
V	1.4	0.75	14.88	51.4	0.91	18.10	62.0

$[\text{Styrene}]_I = 48.97$ mmol, $[\text{ACL}]_I = 48.97$ mmol, $[\text{ACPDA}]_I = 5.0$ mmol, $[\text{M}] = 5$ mmol.

The degree of swelling (%S_w) in polymer beads decreased from 8.65 wt.% to 3.90 wt.% on varying the concentration of divinyl benzene from 0.8% to 2.0% (Table 1). The contents of chlorine in polymer beads varied from 20.59 wt.% to 15.83 wt.%, which was corresponded to 5.80 mmol g^{-1} to 4.46 mmol g^{-1} of allyl chloride (ACL). The decreasing trend in ally chloride in polymer beads on increasing the amount of divinyl benzene was due to competitive copolymerization of divinyl benzene (DVB) and allyl chloride with styrene; hence, the amount of allyl chloride in polymer beads was decreased. This variation in the amount of allyl chloride in polymer beads has ultimately influenced the loading of Schiff base (ACPDA) and metal ions.

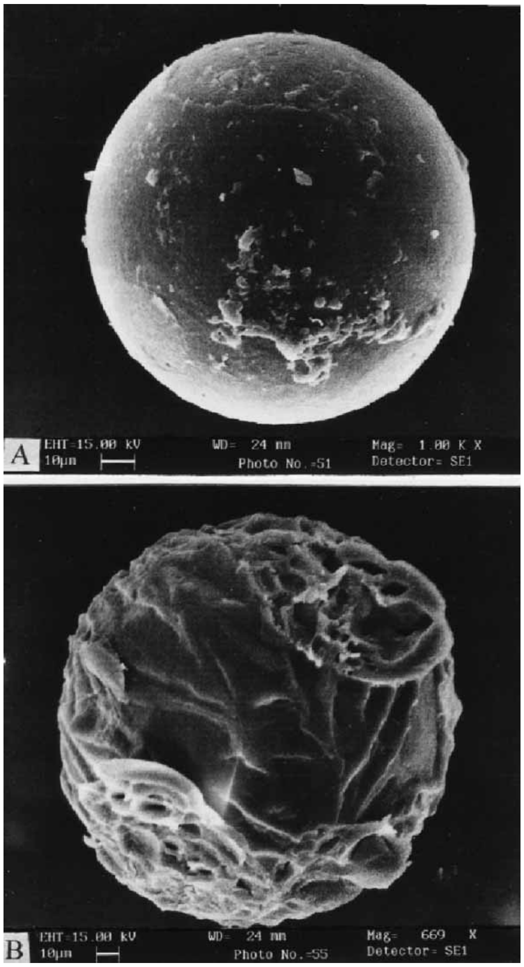

Fig. 1. SEM photographs for polymer beads before (A) and after swelling (B).

3.1 Synthesis of N,N′-bis (acetyl acetone) o-Phenylenediamine Schiff Base and its Loading on Polymer Beads

N,N′-bis (acetyl acetone) o-phenylene diamine Schiff base (ACPDA) was synthesized by reacting, o-phenylene diamine (5 mmol, 0.54 g) with acetyl acetone (10 mmol, 1.0 g), which showed a significant yield of 65 wt.% (Scheme 1). The synthesized ACPDA Schiff base was characterized for its molecular weight (MW) and composition. The MW of Schiff base was 272.4 g mol^{-1}. The composition of Schiff base by elemental analysis corresponded to an empirical formula as $C_{16}H_{20}N_2O_2$. The I.R spectra of Schiff base (ACPDA) given absorption bands at 1626 cm^{-1} and 1576 cm^{-1}, which were due to the presence of >C=N and -C=C- functional groups in the Schiff base. A broad band between 2936 cm^{-1}–3323 cm^{-1} was attributed to phenolic -OH of ACPDA Schiff base (Scheme 1).

The synthesized ACPDA Schiff base was supported on cross-linked polymer beads (Scheme 2) obtained at different concentrations of divinyl benzene (DVB). The amount of supported Schiff base on polymer beads varied with the type of polymer beads obtained at different concentrations of divinyl benzene (Table 2). The elemental analysis of polymer beads showed variation in the content of nitrogen from 4.36–4.20 wt.%, which is corresponding to the variation of ACPDA Schiff base form 1.52 mmol–1.46 mmol on polymer beads (Table 2).

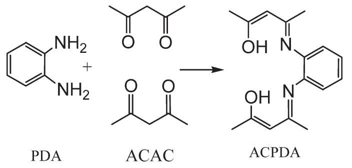

Sch. 1. Synthesis of ACPDA Schiff base.

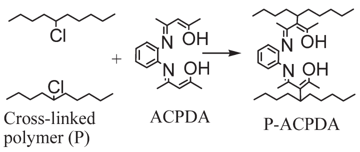

Sch. 2. Loading of ACPDA Schiff base on polymer beads.

The loading of ACPDA Schiff base increased up to a maximum 1.50 mmol concentration of divinyl benzene in polymer beads (Type III), but on further increasing the concentration of divinyl benzene (>1.5 mmol) in polymer beads (Types IV and V), the loading of ACPDA Schiff base was decreased (Table 2). The polymer beads prepared at 1.5 mmol of DVB had a maximum 1.96 mmol of ACPDA Schiff base, but decreased to 1.46 mmol of ACPDA Schiff base at 2.0 mmol concentration of DVB. The Schiff base supported polymer beads were also analyzed for unreacted chlorine, which failed to react with Schiff base either due to steric hindrance of polymer backbone or due to already supported Schiff base on polymer backbone. The content of free chlorine was minimum (3.48 wt.%) in Schiff base supported polymer beads, which were prepared with 1.5 mmol concentration of DVB, which clearly indicated that polymer beads with 1.5 mmol of DVB were suitable to anchor ACPDA Schiff base than polymer beads obtained at high concentration (>1.5 mmol) of divinyl benzene. The anchoring of Schiff base on polymer beads was confirmed by comparing the I.R. spectra of polymer beads with Schiff base supported polymer beads, which showed new absorption bands corresponding to supported Schiff base (Figure 2) and significant reduction in intensity of absorption band at 1262 cm^{-1} for Cl-C group.

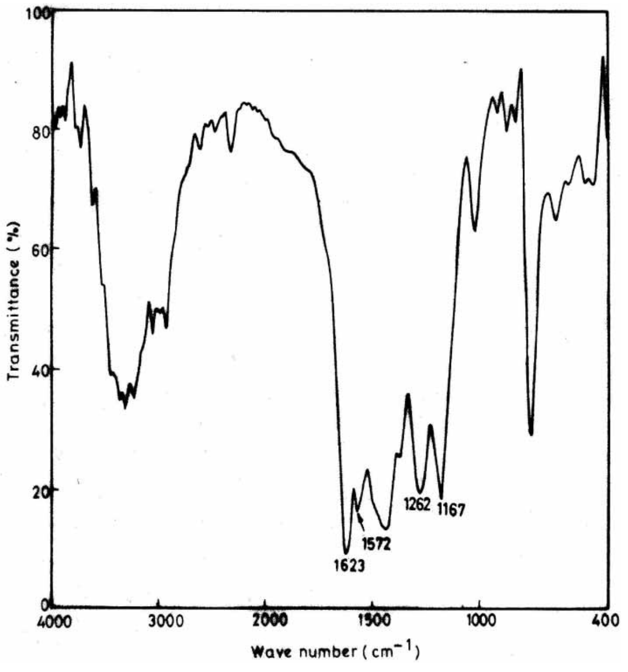

Fig. 2. FTIR spectrum of polymer supported Schiff base (P-ACPDA).

3.2 Loading of Metal Ions on Unsupported and Polymer Supported Schiff Base

The loading of copper(II) and iron(III) ions on Schiff base was carried out refluxing 5.0 mmol of metal ions and 5.0 mmol of Schiff base in DMF solution and complexation of metal ions on polymer supported Schiff base was carried out by refluxing Schiff base supported polymer beads (1.0 g) in DMF solution containing 5.0 mmol of metal ions (Scheme 3). The loading of metal ions on unsupported and polymer supported Schiff base was confirmed by comparing the I.R. spectra of unloaded and metal ions loaded Schiff base complexes.

The I.R. spectra of unsupported Schiff base complexes of copper(II) and iron(III) ions showed absorption bands at 1594 cm^{-1} and 1613 cm^{-1}, respectively for >C=N- group, which appeared at 1626 cm^{-1} in unsupported Schiff base. The absorption band at 1576 cm^{-1} for >C=C< group in unsupported Schiff base was shifted to 1545 cm^{-1} and 1551 cm^{-1} on complexation with copper(II) and iron(III) ions. The polymer supported Schiff base showed absorption bands at 1590 cm^{-1} (>C=N-) and 1540 cm^{-1} (>C=C<) on complexation with copper(II) ions (Figure 3A) and at 1608 cm^{-1} (>C=N-) and 1545 cm^{-1} (>C=C<) on complexation with iron(III) ions (Figure 3B). The unsupported Schiff base on complexation with copper(II) ions showed new bands at 546 cm^{-1} and 435 cm^{-1} due to formation of metal oxygen bond (M-O) and metal nitrogen bond (M-N), whereas the complexation of iron(III) ions showed these new bands at 564 cm^{-1} (M-O) and 440 cm^{-1} (M-N), respectively. The polymer supported Schiff base (P-ACPDA) on complexation with copper(II) ions showed new bands at 542 cm^{-1} (M-O) and 429 cm^{-1} (M-N) (Figure 3A) and on complexation with iron(III) ions, these bands appeared at 559 cm^{-1} (M-O) and 435 cm^{-1}(M-N), respectively (Figure 3B). In addition to these bands, the complexation of metal ions with unsupported and polymer supported Schiff base has suppressed the absorption band corresponding to -OH group, which appeared in unsupported and supported Schiff base. The appearance of new absorption bands and a shift in absorption bands of Schiff base on complexation with metal ions has been used as an evidence to support the coordination of metal ions with phenolic oxygen (-O-M) and azomethyne nitrogen (-C=N-) of Schiff base.

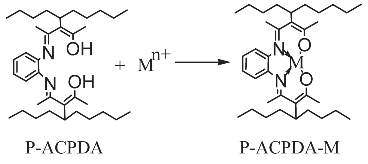

Sch. 3. Loading of metal ions on polymer supported Schiff base.

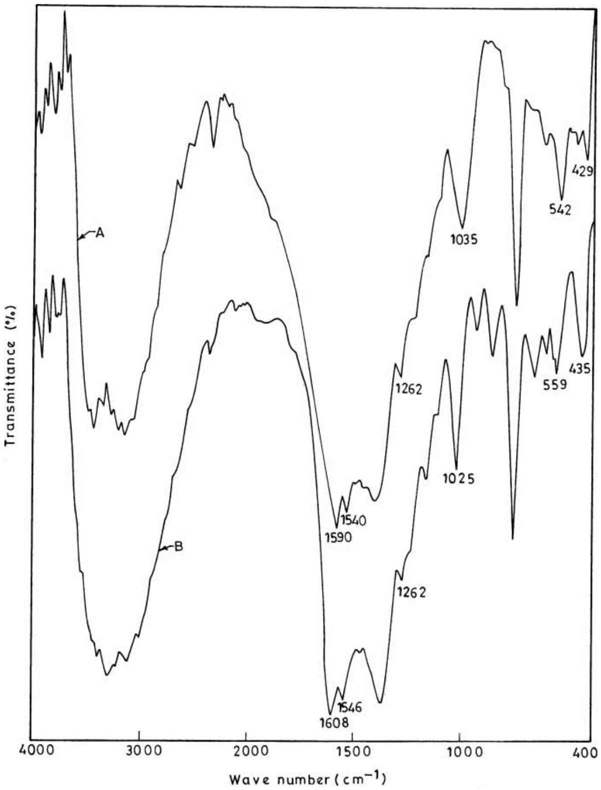

Fig. 3. FTIR spectrum of polymer supported Schiff base complexes of copper(II) (A) and iron(III) (B) ions.

The UV spectra of unsupported and polymer supported Schiff base were also recorded (Table 4), which showed significant variations in $\pi \rightarrow \pi^*$, $n \rightarrow \pi^*$, C → T and d → d transitions on complexation with metal ions in comparison to absorption bands of unsupported and polymer supported Schiff base (Table 4). The variations in transition frequencies in electronic spectra of unsupported and polymer supported Schiff base on complexation with metal ions were also used as evidence to support the complexation of metal ions with unsupported and polymer supported Schiff base. The electronic transitions and magnetic moment (μ) of metal complexes (Table 4) were used to propose the structures of metal complexes of unsupported and polymer supported Schiff base.

The copper(II) ions complexes showed square planar structure, whereas iron(III) ions complexes were having octahedral structure both in unsupported and polymer supported Schiff base (Table 4). The amount of metal ions loaded on unsupported and polymer supported Schiff base varied with the type of metal ions and properties of polymer beads (Table 3).

The loading of copper(II) ions increased initially from 0.85 mmol g^{-1} to 1.38 mmol g^{-1}, but loading of iron(III) ions increased from 0.94 mmol g^{-1} to 1.71 mmol g^{-1} on increasing the amount of divinyl benzene from 0.8 mmol to 1.5 mmol in polymer beads. The polymer beads with a high amount of divinyl benzene (>1.5 mmol) showed a decreasing trend for loading of copper(II) and iron(III) ions (Table 3). Similar trends were shown by efficiency of loading (%EL) and efficiency of complexation (%EC) of metal ions Equations (5) and (6). However, the overall loading of iron(III) ions was higher than copper(II) ions, which was attributed to a high binding affinity of polymer supported Schiff base for iron(III) ions than for copper(II) ions. The beads obtained at high concentration of divinyl benzene (>1.5 mmol) were having low pore volume (V_p) and low cross-link molecular weights (M_c), which was another reason for preventing the Schiff base to anchor on polymer beads (P-ACPDA); hence, these beads showed low metal ions loading than the beads obtained at low concentration of divinyl benzene. The complexation of metal ions has increased the thermal stability of Schiff base as clear from the thermograms recorded for polymer supported Schiff base and its metal complexes (Figure 4).

The polymer supported Schiff base (P-ACPDA) showed 57% weight loss at 550°C, but its copper(II) and iron(III) ions complexes showed a weight loss of 29.2% and 21.3%, respectively at the same temperature (Figure 4). This trend in weight loss has clearly indicated that the complexation of metal ions has increased the thermal stability of Schiff base and iron(III) ions complexes become more stable than the complexes of copper(II) ions.

The characteristics of the synthesized polymer beads have clearly indicated that polymer beads prepared with 1.5 mmol of divinyl benzene (Type III) had optimum properties for loading of Schiff base and metal ions; hence, these beads were used to evaluate their catalytic activity in decomposition

Table 4. Electronic and magnetic properties of unsupported (ACDPA-M) and polymer supported metal complexes (P-ACPDA-M) of ACDPA Schiff base

Type of complex	$\pi \rightarrow \pi^*$/nm	$n \rightarrow \pi^*$/nm	C → T/nm	d → d/nm	μ/BM	Structure of complexes
ACPDA	270	306	—	—	—	—
P-ACPDA	268	303	—	—	—	—
ACPDA-Cu (II)	217	277	284	334	1.91	Square planar
P-ACDPA-Cu (II)	214	275	282	332	1.92	-do-
ACPDA-Fe (III)	259	270	354	428	5.78	Octahedral
P-ACDPA-Fe (III)	256	267	349	425	5.80	-do-

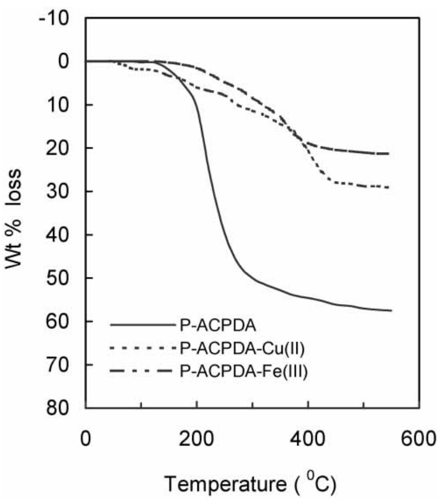

Fig. 4. Percent weight loss in polymer supported Schiff base and its metal complexes.

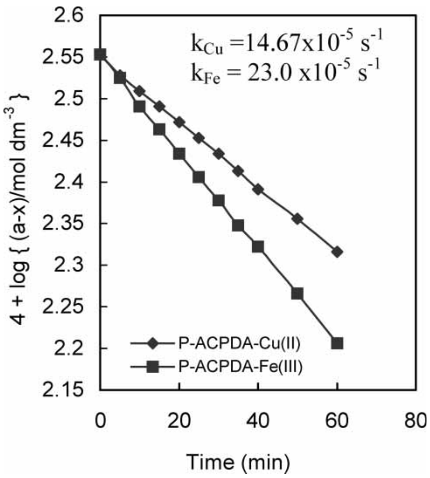

Fig. 5. The decomposition of hydrogen peroxide in presence of polymer supported metal complexes.

of hydrogen peroxide in comparison to unsupported Schiff base complexes of copper(II) and iron(III) ions.

3.3 Decomposition of Hydrogen Peroxide

To evaluate the effect of polymer support on activity of metal complexes, the decomposition of hydrogen peroxide was studied in presence of unsupported and polymer supported metal complexes. The decomposition of hydrogen peroxide was studied under different experimental conditions and kinetic parameters were estimated for unsupported and polymer supported complexes of metal ions. To evaluate the catalytic activity of polymer supported metal complexes, the polymer beads were swollen in DMF for 24 h so that the activity of polymer loaded metal complexes was utilized properly in decomposition of hydrogen peroxide. The decomposition of hydrogen peroxide increased linearly in the presence of polymer supported complexes of copper(II) and iron(III) ions with the progress of reaction time as is clear from the plot drawn between log (a-x) vs. reaction time (Figure 5) at constant concentration of hydrogen peroxide (3.54×10^{-2} mol dm^{-3}) and catalyst. The rate of decomposition of hydrogen peroxide was higher with polymer supported Schiff base complexes of iron(III) ions (P-ACPDA-Fe) than complexes of copper(II) ions (P-ACPDA-Cu). The linear variation for log(a-x) with reaction time (Figure 5) has indicated clearly that the decomposition of hydrogen peroxide has followed first order kinetics. The same trend was observed with unsupported metal complexes and uncatalyzed decomposition of hydrogen peroxide. The rate constant (*k*) for decomposition of hydrogen peroxide in presence of Schiff base complexes of iron(III) and copper (II) ions was evaluated and found to be 23×10^{-5} s^{-1} and 14.67×10^{-5} s^{-1}, respectively.

The decomposition of hydrogen peroxide was also studied using unsupported complexes of iron(III) and copper(II) ions at 25°C from which it was clear that the rate of decomposition of hydrogen peroxide was higher with polymer supported metal complexes than unsupported metal complexes (Table 5 and Figure 5). The rate of decomposition of hydrogen peroxide (Rp) was also studied at different concentrations of hydrogen peroxide using unsupported and polymer supported Schiff base complexes of copper(II) and iron(III) ions. The effect of hydrogen peroxide concentration on its decomposition was studied by varying its concentration from 1.79×10^{-2} mol dm^{-3} to 5.96×10^{-2} mol dm^{-3} at a constant concentration of copper(II) (13.8×10^{-4} mol dm^{-3}) and iron(III) ions (17.1×10^{-4} mol dm^{-3}) in the reaction mixture. The log-log plots were drawn between the rate of

Table 5. Comparison of rate constant (*k*), energy of activation (*Ea*) and turnover number (TON) for catalytic decomposition of hydrogen peroxide

Type of complex	$k \times 10^5/\text{s}^{-1}$	TON $\times 10^{-20}$/ molecules mol^{-1} s^{-1}	*Ea*/ k J mol^{-1}
ACPDA-Cu (II)	0.20	0.29	54.53
P-ACDPA-Cu (II)	14.67	23.67	41.36
ACPDA-Fe (III)	0.35	0.43	51.76
P-ACDPA-Fe (III)	23.0	29.91	35.26

$[H_2O_2] = 3.54 \times 10^{-4}$ mol dm^{-3}, $[Cu(II)] = 13.8 \times 10^{-4}$ mol dm^{-3}, $[Fe(III)] = 17.1 \times 10^{-4}$ mol dm^{-3}, Temp. = 25°C, $\mu = 0.2$ mol dm^{-3}, beads (Type-III).

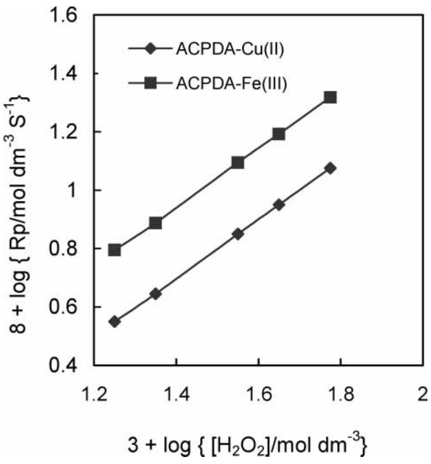

Fig. 6. Effect of hydrogen peroxide concentration on its rate of decomposition in presence of unsupported metal complexes.

decomposition of hydrogen peroxide (Rp) and concentration of hydrogen peroxide using unsupported (Figure 6) and polymer supported metal complexes (Figure 7).

The rate of decomposition of hydrogen peroxide varied linearly with the initial concentration of hydrogen peroxide with unsupported (Figure 6) and supported metal complexes of Schiff base (Figure 7), which was a clear indication for first order kinetic for decomposition of hydrogen peroxide with initial concentration of hydrogen peroxide. Although the application of polymer support has increased the rate of decomposition of hydrogen peroxide, the mechanism for decomposition of hydrogen peroxide was the same with unsupported and polymer supported metal complexes.

The increased rate of decomposition (Rp) of hydrogen peroxide with polymer supported metal complexes (P-ACPDA-M) was due to the increased activity of metal ions on polymer support than activity of unsupported metal ions (ACPDA-M) in decomposition of hydrogen peroxide, which clearly indicated that polymer support has played a significant role in controlling the activity of metal complexes.

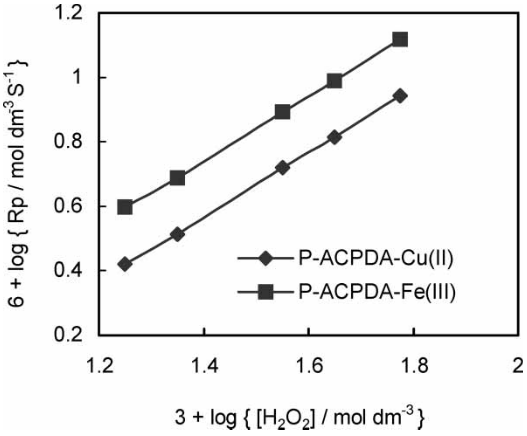

Fig. 7. Effect of hydrogen peroxide concentration on its decomposition in the presence of polymer supported metal complexes.

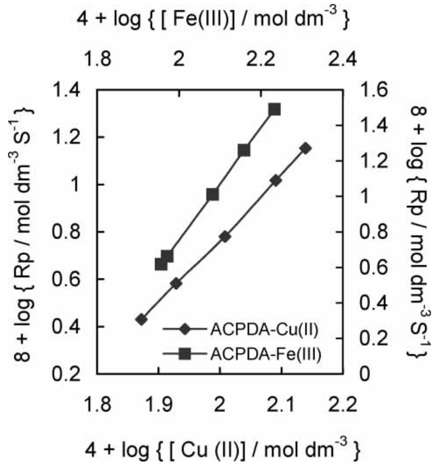

Fig. 8. Effect of concentration of unsupported metal complexes on rate of decomposition of hydrogen peroxide.

The effect of metal ions concentration on decomposition of hydrogen peroxide was determined by varying the concentration of copper(II) ions from 7.5×10^{-4} mol dm^{-3} -13.8×10^{-4} mol dm^{-3} and iron(III) ions from 9.1×10^{-4} mol dm^{-3}–17.1×10^{-4} mol dm^{-3} at a constant concentration of hydrogen peroxide (3.54×10^{-2} mol dm^{-3}) and ionic strength ($\mu = 0.2$ mol dm^{-3}) of the medium. The solution pH was fixed as 7.5 and 6.8 for studying the decomposition hydrogen peroxide in presence of Schiff base complexes of iron(III) and copper(II) ions, respectively. The log-log plots drawn between rate of decomposition of hydrogen peroxide (Rp) Vs concentration of unsupported (Figure 8) and polymer supported metal complexes (Figure 9) have clearly indicated that the rate of decomposition of hydrogen peroxide (Rp) varied linearly in homogeneous (Figure 8) and heterogeneous conditions (Figure 9). The comparison of rate of decomposition (Rp) of hydrogen peroxide with unsupported (Figure 8) and

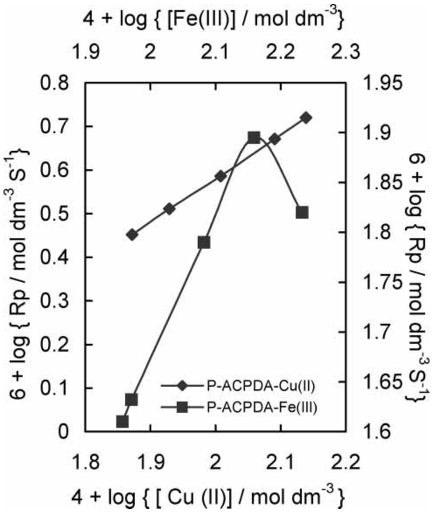

Fig. 9. Effect of concentration of polymer supported metal complexes on the rate of decomposition of hydrogen peroxide.

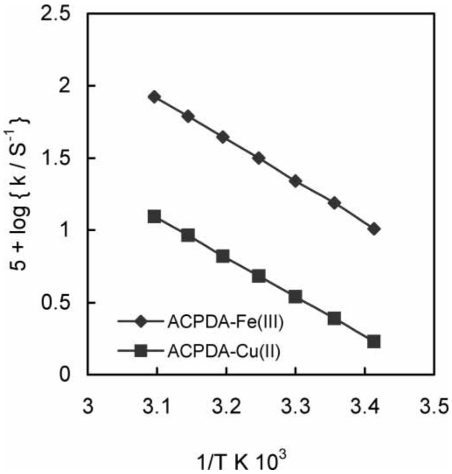

Fig. 10. Energy of activation (*Ea*) for decomposition of hydrogen peroxide with unsupported metal complexes of Schiff base.

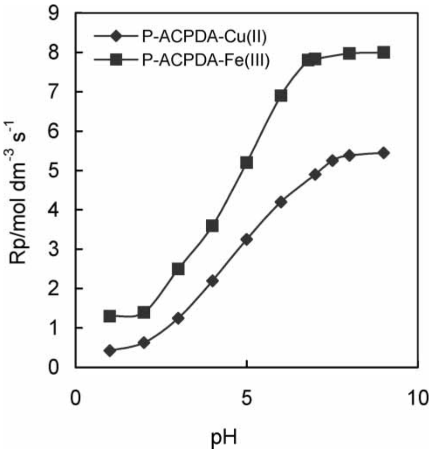

Fig. 12. Effect of solution pH on decomposition of hydrogen peroxide in the presence of polymer supported metal complexes of Schiff base.

polymer supported metal complexes (Figure 9) has clearly indicated that the rate of decomposition of hydrogen peroxide was higher with polymer supported metal complexes than unsupported metal complexes. The low rate of decomposition of hydrogen peroxide with unsupported metal complexes was due to the deactivation of catalyst and lack of proper orientations as was possible with polymer supported metal complexes.

The polymer supported metal complexes were more efficient and active in decomposition of hydrogen peroxide than unsupported metal complexes, which was clear from the values of the turn over number (TON) for supported and unsupported metal complexes (Table 5). The Schiff base complexes on polymer support showed a high turnover number for copper(II) and iron(III) ions in comparison to unsupported metal complexes. The catalytic activity of iron(III) ions on polymer support was low at its high concentration (17.1×10^{-4} mol dm^{-3}) than the activity of Schiff base complexes of copper(II) ions on polymer support at same concentration (Figure 9).

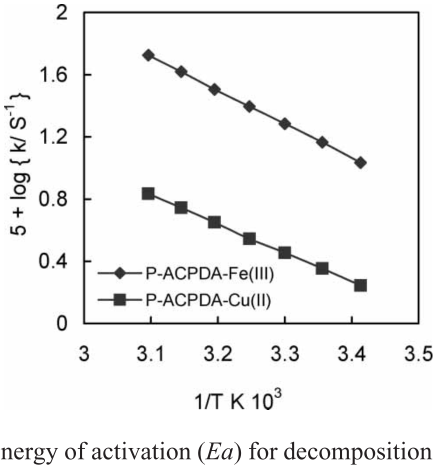

Fig. 11. Energy of activation (*Ea*) for decomposition of hydrogen peroxide with polymer supported metal complexes of Schiff base.

The deviation in rate of decomposition of hydrogen peroxide at high concentration of polymer supported iron(III) ions complexes (17.1×10^{-4} mol dm^{-3}) was due to the decrease in rate of diffusion of hydrogen peroxide in polymer beads, but polymer supported complexes of copper(II) ions provided no limitation on diffusion of hydrogen peroxide; hence, the rate of decomposition (Rp) of hydrogen peroxide continued to increase on increasing the amount of Schiff base complexes of copper(II) ions on polymer support (Figure 9).

These data have clearly indicated that the activity of Schiff base complexes of metal ions increased on polymer support and rate of decomposition (Rp) of hydrogen peroxide followed first order kinetics with a concentration of unsupported and polymer supported Schiff base complexes of metal ions (Figures 8 and 9).

3.4 Effect of Temperature and Solution pH

The rate of decomposition of hydrogen peroxide was studied at different temperatures ranging from 20°C to 50°C using unsupported (ACPDA-M) and polymer supported Schiff base complexes of metal ions (P-ACPDA-M) at a constant concentration of hydrogen peroxide (3.54×10^{-2} mol dm^{-3}) and catalyst and rate constant (k) for decomposition of hydrogen peroxide was determined. The energy of activation (*Ea*) for decomposition of hydrogen peroxide was determined by drawing an Arrhenius plot between log k vs. inverse of reaction temperature (Figures 10 and 11). The rate constant (k) for decomposition of hydrogen peroxide increased on increasing the reaction temperature from 20°C to 50°C. The rate of decomposition of hydrogen peroxide with polymer supported Schiff base complexes of metal ions was higher (Figure 11) than unsupported Schiff base metal complexes of metal ions (Figure 10). The energy of activation (*Ea*) for decomposition of hydrogen peroxide was lowest

(35.26 kJ mol^{-1}) with polymer supported Schiff base complexes of iron(III) ions (Figure 11) and was highest (54.53 kJ mol^{-1}) with unsupported Schiff base complexes of copper(II) ions (Figure 10).

In general, the energy of activation for decomposition of hydrogen peroxide was low with polymer supported Schiff base complexes of metal ions in comparison to unsupported Schiff base complexes (Table 5, Figures 10 and 11), which clearly indicated that polymer support has decreased the energy of activation for decomposition of hydrogen peroxide by creating a suitable microenvironment (13) around active sites that was missing with unsupported Schiff base complexes of metal ions.

The rate of decomposition of hydrogen peroxide was also studied in a solution of different pH using unsupported and polymer supported Schiff base complexes of metal ions at a constant concentration of hydrogen peroxide (3.54×10^{-2} mol dm^{-3}) and catalyst (Figure 12).

The rate of decomposition of hydrogen peroxide (Rp) in the presence of unsupported and polymer supported metal complexes showed a significant increase with solution pH and also showed higher activity than unsupported Schiff base complexes. The polymer supported Schiff base complexes of iron(III) ions showed an increasing trend in the rate of decomposition of hydrogen peroxide up to a solution pH of 6.8, but Schiff base complexes of copper(II) ions showed an increasing trend up to pH 7.5 (Figure 12). Similar trends were shown by unsupported Schiff base complexes of metal ions in decomposition of hydrogen peroxide on varying the solution pH. This variation in the rate of decomposition of hydrogen peroxide with solution pH was indicative of an adverse effect of hydrogen ions in decomposition of hydrogen peroxide in the presence of Schiff base complexes of metal ions; hence, the rate of decomposition was increased on increasing the solution pH. Since the unsupported and polymer supported Schiff base complexes of metal ions showed a similar trend in the rate of decomposition of hydrogen peroxide on varying solution pH; hence, it is assumed that the decomposition of hydrogen peroxide followed similar steps with unsupported and supported Schiff base complexes of metal ions as proposed in Equations (7–10).

$$H_2O_2 \xrightarrow{k_d} H^+ + HOO^- \tag{7}$$

$$(M(ACPDA)_2) + {}^-OOH \xleftrightarrow{K} (M(ACPDA)_2OOH)^- \tag{8}$$

$$\begin{aligned}&(M(ACPDA)_2OOH)^- \xrightarrow[\text{SLOW}]{k_1} (M(ACPDA)_2)\\ &+\frac{1}{2}O_2 + {}^-OH\end{aligned} \tag{9}$$

$${}^-OH + H^+ \xrightarrow[\text{Fast}]{k_1'} H_2O \tag{10}$$

On considering Equations (7–10), the rate expression for decomposition of hydrogen peroxide was derived as in Equation (11).

$$\frac{-d[H_2O_2]}{dt} = \frac{k_d K k_1 [M(ACPDA)_2][H_2O_2]}{[H^+]} \tag{11}$$

Where, k_d and k_1 are the rate constants for dissociation of hydrogen peroxide and intermediate complex (M(ACPDA)$_2$ $^-$OOH) formed by the association of $^-$OOH ions with Schiff base complexes of metal ions, K is the equilibrium constant for the formation of intermediate complex between $^-$OOH and Schiff base complex of metal ions (M (ACPDA)$_2$). Equation (11) showed significant agreement with the rate of decomposition of hydrogen peroxide with a concentration of hydrogen peroxide, Schiff base complexes of metal ions and hydrogen ions, which supported the validity of reaction steps as proposed Equations (7–10) for unsupported and supported Schiff base complexes of metal ions.

4 Conclusions

The polymer supported Schiff base complexes of copper(II) and iron(III) ions were prepared successfully by anchoring synthesized N,N′-bis (acetyl acetone)o-phenylene diamine Schiff base (ACPDA) on divinyl benzene (DVB) cross-linked polystyrene beads. The loading capacity of polymer beads for Schiff base and metal ions showed variations with a degree of cross-linking, pore volume (V_p) and cross-link molecular weights (M_c). The size and degree of swelling of polymer beads has varied with varying the degree of cross-linking in polymer beads. These physical characteristics of polymer beads played a significant role in the rate of decomposition of hydrogen peroxide. The rate of hydrogen peroxide decomposition at different concentrations of hydrogen peroxide and catalyst was used to determine the dependence of a reaction rate on these reactants. The polymer support has also played a significant role in reducing the energy of activation for decomposition of hydrogen peroxide in comparison to unsupported Schiff base complexes of metal ions.

5 Acknowledgment

The authors are thankful to I.I.T. Roorkee for providing excellent research facilities to carry out these investigations.

6 References

1. Fukuda, Y., Miura, Y. and Sone, K. (1977) *Bull. Chem. Soc. Jpn.*, **50**, 142.
2. Naga, N.T., Fukuda, Y. and Sone, K. (1977) *Bull. Chem. Soc. Jpn.*, **50**, 154.

3. Linden, G.L. and Farona, M.F. (1977) *J. Catal.*, **48**, 284.
4. Wang, J., Liu, Z., Wang, D. and Guo, D. (2000) *Polym. Int.*, **49**, 1665.
5. Huang, G., Can-Cheng, G. and Si-Si, T. (2007) *J. Mol. Catal. A: Chemical*, **261**, 125.
6. Sherrington, D.C. (1988) *Pure Appl. Chem.*, **60**, 401.
7. Hanková, L., Holub, L. and Jeřábek, K. (2006) *React. and Funct. Polym.*, **66**, 592–598.
8. Vassilev, K., Stamenova, R. and Tsvetanov, C. (2000) *React. and Funct. Polym.*, **46**, 165.
9. Arnold, U., Fan, F., Habicht, W. and Döring, M. (2007) *J. Catal.*, **245**, 55.
10. Chengyau, K., Quing, Y., Aiguo, L. and Xiangzheng, K. (1996) *Polym. Adv. Technol.*, **7**, 76.
11. Guang, Y., Quian, C., Hui, Z., Xuequan, Z.J. and Baotong, H. (1996) *J. Polym. Sci. Polym. Chem. Ed.*, **34**, 2237.
12. Caze, C. (1995) *React. and Funct. Polym.*, **26**, 35.
13. Alxandratos, S.D. and Miller, D.H.J. (2000) *Macromolecules*, **33**, 2001.
14. Henkova, L., Holub, L. and Jerabek, K. (2006) *React. and Funct. Polym.*, **66**, 592.
15. Merrifield, R.B. (1963) *J. Am. Chem. Soc.*, **85**, 2149.
16. Zu-Xing, C., Guo-Yu, X., Gui-Chun, Y. and Wei, W. (2004) *React. and Funct. Polym.*, **61**, 139.
17. Markus, H., Mäki-Arvela, P., Kumar, N., Heikkilä, T., Vesa-Pekka, L., Sjöholm, R., Holmbom, B., Salmi, T. and Murzin, D.Y. (2006) *J. Catal.*, **238**, 301.
18. Kresge, C.T., Leonowicz, M.E., Roth, W.J., Vertuli, J.C. and Beck, J.S. (1992) *Nature*, **35**, 710.
19. Hutchings, G., Page, P. and Hancock, F. (1997) *Chem. Br.*, **33**, 46.
20. Tatiana, L., Wladimir, S., Diana, H., Olaf, K. and Helmut, P. (2007) *J. Mol. Catal. A: Chemical*, **261**, 16.
21. Yoon, J.W., Jong-San, C., Hee-Du, L., Tae-Jin, K. and Jhung, S.H. (2006) *J. Mol. Catal. A: Chemical*, **260**, 181.
22. Fahad, A., Zhibin, Y. and Shiping, Z. (2003) *Macromol. Chem. Phys.*, **29**, 653.
23. Pittman, C.U. Jr., and Ng, Q. (1978) *J. Organomet. Chem.*, **85**, 153.
24. Grubbs, R.H. and Kroll, L.C. (1971) *J. Am. Chem. Soc.*, **93**, 3062.
25. Huidong, Z., Yanmei, Z. and Can, L. (2005) *Tetrahedron Asym.*, **16**, 2417.
26. Grubbs, R.H., Kroll, L.C. and Sweets, E.M. (1973) *J. Macromol. Sci. Chem.,*, **A7**, 1047.
27. Alexandra, T. and Zehavi, U. (1966) *React. and Funct. Polym.*, **31**, 11.
28. Wahlen, J., Hertogh, S.D., De Vos, D.E., Nardello, V., Bogaert, S., Aubry, J.M., Alsters, P.L. and Jacobs, P.A. (2005) *J. Catal.*, **233**, 422.
29. Chisen, J.C., Chisen, J. and Clark, J.H. (1998) *New J. Chem.*, **22**, 81.
30. Brunel, D., Moreau, P., Renzo, F.D., Galaneau, A. and Fazula, F. (1998) *Coord. Chem. Rev.*, **178**, 1055.
31. Luis, S.V., Burgete, M.I. and Altava, B. (1995) *React. and Funct. Polym.*, **26**, 75.
32. Gould, E.S., Hialt, R.H. and Irwin, O.K.C. (1968) *J. Am. Chem. Soc.*, **90**, 4573.
33. Johnson, N.A. and Gould, E.S. (1974) *J. Org. Chem.*, **39**, 407.
34. Janiac, J., Sxharmann, T.G. and Lange, C.H. (1994) *Makramol. Rapid. Commun.*, **15**, 655.
35. Mitani, K., Hayakowa, M. and Yamada, T. (1996) *Makromol. Chem. Phys.*, **197**, 1545.
36. Yongxin, Q., Tao, T., Zhongfu, Z. and Baotong, H. (2003) *J. Polym. Sci. Part A: Polym. Chem.*, **41**, 3313.
37. Gupta, K.C., Abdulkadir, H.K. and Chand, S. (2003) *J. Mol. Catal. A: Chemical*, **202**, 253.
38. Radi, S., Ramadani, A., Lekchiri, Y., Morcellet, M., Crini, G., Janus, L. and Martel, B. (2000) *J. Appl. Polym. Sci.*, **78**, 2495.
39. Yeh, H.C., Eichiger, B.E. and Anderson, N.H. (1981) *Polym. Prepr. Polym. Div. Am. Chem. Soc.*, **22**, 184.